PASJ: Publ. Astron. Soc. Japan **62**, L55–L60, 2010 December 25

Bright X-Ray Flares from the BL Lac Object Markarian 421, Detected with MAXI in 2010 January and February

Naoki ISOBE,[1] Kousuke SUGIMORI,[2] Nobuyuki KAWAI,[2,3] Yoshihiro UEDA,[1] Hitoshi NEGORO,[4] Mutsumi SUGIZAKI,[3] Masaru MATSUOKA,[3,5] Arata DAIKYUJI,[6] Satoshi EGUCHI,[1] Kazuo HIROI,[1] Masaki ISHIKAWA,[5] Ryoji ISHIWATA,[4] Kazuyoshi KAWASAKI,[5] Masashi KIMURA,[7] Mitsuhiro KOHAMA,[3,5] Tatehiro MIHARA,[3] Sho MIYOSHI,[4] Mikio MORII,[2] Yujin E. NAKAGAWA,[3] Satoshi NAKAHIRA,[8] Motoki NAKAJIMA,[9] Hiroshi OZAWA,[4] Tetsuya SOOTOME,[3] Motoko SUZUKI,[3] Hiroshi TOMIDA,[5] Hiroshi TSUNEMI,[7] Shiro UENO,[5] Takayuki YAMAMOTO,[3] Kazutaka YAMAOKA,[8] Atsumasa YOSHIDA,[8] and the MAXI TEAM

[1]*Department of Astronomy, Kyoto University, Kitashirakawa, Oiwake-cho, Sakyo-ku, Kyoto 606-8502*
n-isobe@kusastro.kyoto-u.ac.jp
[2]*Department of Physics, Tokyo Institute of Technology, 2-12-1 Ookayama, Meguro-ku, Tokyo 152-8551*
[3]*Coordinated Space Observation and Experiment Research Group, Institute of Physical and Chemical Research (RIKEN), 2-1 Hirosawa, Wako, Saitama 351-0198*
[4]*Department of Physics, Nihon University, 1-8-14 Kanda-Surugadai, Chiyoda-ku, Tokyo 101-8308*
[5]*ISS Science Project Office, Institute of Space and Astronautical Science (ISAS), Japan Aerospace Exploration Agency (JAXA), 2-1-1 Sengen, Tsukuba, Ibaraki 305-8505*
[6]*Department of Applied Physics, University of Miyazaki, 1-1 Gakuen Kibanadai-nishi, Miyazaki, Miyazaki 889-2192*
[7]*Department of Earth and Space Science, Osaka University, 1-1 Machikaneyama, Toyonaka, Osaka 560-0043*
[8]*Department of Physics and Mathematics, Aoyama Gakuin University, 5-10-1 Fuchinobe, Chuo-ku, Sagamihara 252-5258*
[9]*School of Dentistry at Matsudo, Nihon University, 2-870-1 Sakaecho-nishi, Matsudo, Chiba 101-8308*

(Received 2010 June 3; accepted 2010 October 1)

Abstract

Strong X-ray flares from the blazar Mrk 421 were detected in 2010 January and February through 7-month monitoring with the MAXI GSC. The maximum 2–10 keV flux in the January and February flares was measured to be 120 ± 10 mCrab and 164 ± 17 mCrab, respectively; the latter is the highest among those reported from the object. A comparison of the MAXI and Swift BAT data suggests a convex X-ray spectrum with an approximated photon index of $\Gamma \gtrsim 2$. This spectrum is consistent with a picture that MAXI is observing near the synchrotron peak frequency. The source exhibited a spectral variation during these flares, slightly different from those in previous observations, in which the positive correlation between the flux and hardness was widely reported. By equating the halving decay timescale in the January flare, $t_{\rm d} \sim 2.5 \times 10^4$ s, to the synchrotron cooling time, the magnetic field was evaluated to be $B \sim 4.5 \times 10^{-2}\,{\rm G}\,(\delta/10)^{-1/3}$, where δ is the jet beaming factor. Assuming that the light crossing time of the emission region is shorter than the doubling rise time, $t_{\rm r} \lesssim 2 \times 10^4$ s, the region size was roughly estimated as $R < 6 \times 10^{15}\,{\rm cm}\,(\delta/10)$. These results are consistent with values previously reported. For the February flare, the rise time, $t_{\rm r} < 1.3 \times 10^5$ s, gives a loose upper limit on the size as $R < 4 \times 10^{16}\,{\rm cm}\,(\delta/10)$, although the longer decay time, $t_{\rm d} \sim 1.4 \times 10^5$ s, indicates $B \sim 1.5 \times 10^{-2}\,{\rm G}\,(\delta/10)^{-1/3}$, which is weaker than the previous results. This could be reconciled by invoking a scenario that this flare is a superposition of unresolved events with a shorter timescale.

Key words: BL Lacertae objects: individual (Markarian 421) — galaxies: active — radiation mechanisms: non-thermal — X-rays: galaxies

1. Introduction

Blazars, including BL Lacertae (BL Lac) objects, are a class of active galactic nuclei (AGN), from which a relativistic jet is emanating close to our line of sight. In addition to their non-thermal radiation ranging from the radio to gamma-ray frequencies, and strong polarization at radio and optical frequencies, one of the most outstanding characteristics of blazars is their rapid and high-amplitude intensity variations or flares, which provide clues about the flow dynamics, as well as to particle acceleration and cooling processes operating in the jet. Since the Ginga (e.g., Sembay et al. 1993; Tashiro et al. 1995) and ASCA era (e.g., Takahashi et al. 2000; Tanihata et al. 2001), X-ray observations have been one of the most useful tools to study the variability of blazars. In addition, remarkable progress was successively accomplished by X-ray observations with RXTE and Swift observations (e.g., Kataoka et al. 2001; Tramacere et al. 2009).

Located at a redshift of $z = 0.031$, Mrk 421 is a high-energy peaked BL Lac object (HBLs: Padovani & Giommi 1995). The object is one of the brightest extragalactic sources at very high energy (VHE) gamma-rays above $\sim$100 GeV (Punch et al. 1992). A number of studies (e.g., Kino et al. 2002) revealed that the multi-frequency spectral energy distribution (SED)

of the source and its variation are basically well understood within the framework of a simple one-zone synchrotron-self-Compton (SSC) model (Band & Grindlay 1985). For Mrk 421, the X-ray and VHE gamma-ray bands correspond to, or are located slightly above, the peak frequencies of the synchrotron and inverse Compton (IC) spectral components, respectively. As a result, Mrk 421 is one of the most extensively studied blazars in the X-ray band (e.g., Takahashi et al. 2000; Tanihata et al. 2004), and X-ray flares were frequently reported (e.g., Tramacere et al. 2009; Donnarumma et al. 2009).

As the first astronomical mission on the Exposed Facility of the Japanese Experiment Module "Kibo", attached to the International Space Station (ISS), Monitor of All-sky X-ray Image (MAXI: Matsuoka et al. 2009) started its operation in 2009 August. Thanks to its unprecedentedly high sensitivity as an all-sky X-ray monitor, and to its capability of real-time data transfer, MAXI is able not only to make a continuous monitor of X-ray sources including AGN, but also to quickly alert us to various transient X-ray phenomena (Negoro et al. 2010), like flares of blazars. Actually, in the 7-month MAXI observation, we successfully alerted two strong X-ray flares from Mrk 421 (Isobe et al. 2010a, 2010b); in one of these flares the object exhibited the highest X-ray flux among those ever recorded. In the present paper, we report on the X-ray features of Mrk 421 in these flares, and discuss their implication.

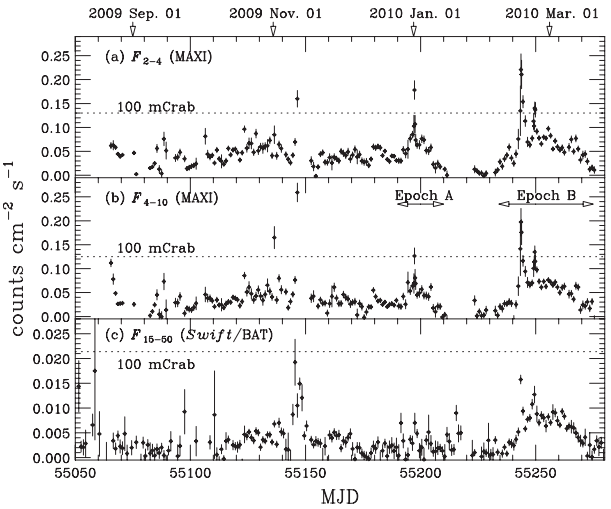

Fig. 1. Daily lightcurve of Mrk 421. Panels (a) and (b) show the normalized count rates in the 2–4 keV (F_{4-10}) and 4–10 keV (F_{2-4}) ranges, respectively, measured with the MAXI GSC from 2009 August 22 (MJD = 55062) to 2010 March 20 (MJD = 55275). For MJD = 55197, 55243, and 55249, F_{4-10} and F_{2-4} are plotted in a time resolution of 6 hours, in order to resolve the peak. The Swift BAT lightcurve in 15–50 keV, F_{15-50}, is plotted in panel (c). All errors represent the 1σ statistical one. The dotted lines indicate the count rate of 100 mCrab in the individual energy ranges. The two arrows in the center panel define Epochs A and B.

2. Observation and Results

Among the two X-ray instruments onboard MAXI, the Gas Slit Camera (GSC) and the Solid-state Slit Camera (Tsunemi et al. 2010), we analyze only the GSC data in the present paper, because of its higher sensitivity and sky coverage ($\sim$97% per day). The GSC utilizes 12 position-sensitive large-area proportional counters sensitive to X-ray photons in 2–20 keV, although 4 out of them were switched off, on 2009 September 22, due to unexpected discharge events.

The MAXI GSC signals from Mrk 421 were integrated orbit by orbit within a $3^\circ \times 3^\circ$ square aligned to the scan direction centered on the source, while the background level was evaluated from two squares with offsets of $\pm 3^\circ$ toward the scan direction on the sky, of which the size was same as that of the source region. We normalized the background-subtracted signal counts by a time-integrated effective area of the collimator plus slits above the proportional counters. In the following, the data from all the activated counters are summed up.

As assistance for interpreting the MAXI GSC data, we utilized hard X-ray data taken with the Burst Alert Telescope (BAT: Barthelmy et al. 2005) onboard Swift. Swift BAT is composed of a coded aperture mask and large area (5200 cm^2) CdZnTe detectors. Thanks to its wide field of view ($\sim$1.4 str), the typical sky coverage of the instrument exceeds $\sim$70% (Krimm 2006) in a one-day observation. The daily Swift BAT lightcurves of Mrk 421 in the 15–50 keV range are available from the Swift BAT transient monitor results[1], provided by the Swift BAT team.

Figures 1a and 1b show the normalized signal count rates from Mrk 421 derived with the MAXI GSC in 2–4 keV and 4–10 keV, F_{2-4} and F_{4-10}, respectively, from 2009 August 22 (MJD = 55065) to 2010 March 20 (MJD = 55275). In the plot, 10% of the count rate from the Crab Nebula (100 mCrab, $F_{2-4} = 0.13$ counts cm^{-2} s^{-1} and $F_{4-10} = 0.125$ counts cm^{-2} s^{-1}: Nakahira et al. 2010) is indicated by dotted lines. We have noticed some relatively long data gaps, such as on 2009 September 3–7 (MJD = 55077–55081), November 12–16 (MJD = 55147–55151), and 2010 January 19–26 (MJD = 55215–55222). During these periods, Mrk 421 was located in the direction toward the ISS orbital pole unobservable with the MAXI GSC. The Swift BAT lightcurve in the 15–50 keV range F_{15-50} is compared in figure 1c.

The lightcurve reveals that Mrk 421 is highly variable in all of the energy ranges. The fractional root-mean-square variability parameters (e.g., Rodríguez-Pascual et al. 1997) in F_{2-4}, F_{4-10}, and F_{15-50} were evaluated to be 0.52, 0.71, and 0.70, respectively, from the daily averaged lightcurves. The GSC has detected at least four flares with an X-ray flux of $\gtrsim$100 mCrab, on 2009 November 1 (MJD = 55136), 2009 November 11 (MJD = 55146), 2010 January 1 (MJD = 55197: Isobe et al. 2010a), and February 16 (MJD = 55243: Isobe et al. 2010b). Unfortunately, the observational conditions for the first and second flares were found to be relatively bad, although the second flare appears to be concurrent with the hard X-ray one, detected with the Swift BAT on 2009 November 10 (MJD = 55145: Krimm et al. 2009). Therefore, we focus on the GSC data associated with the third and forth flares, which are indicated by two arrows, denoted as **Epoch A** and **Epoch B**, respectively, in figure 1b. During Epoch A,

[1] ⟨http://heasarc.gsfc.nasa.gov/docs/swift/results/transients/⟩.

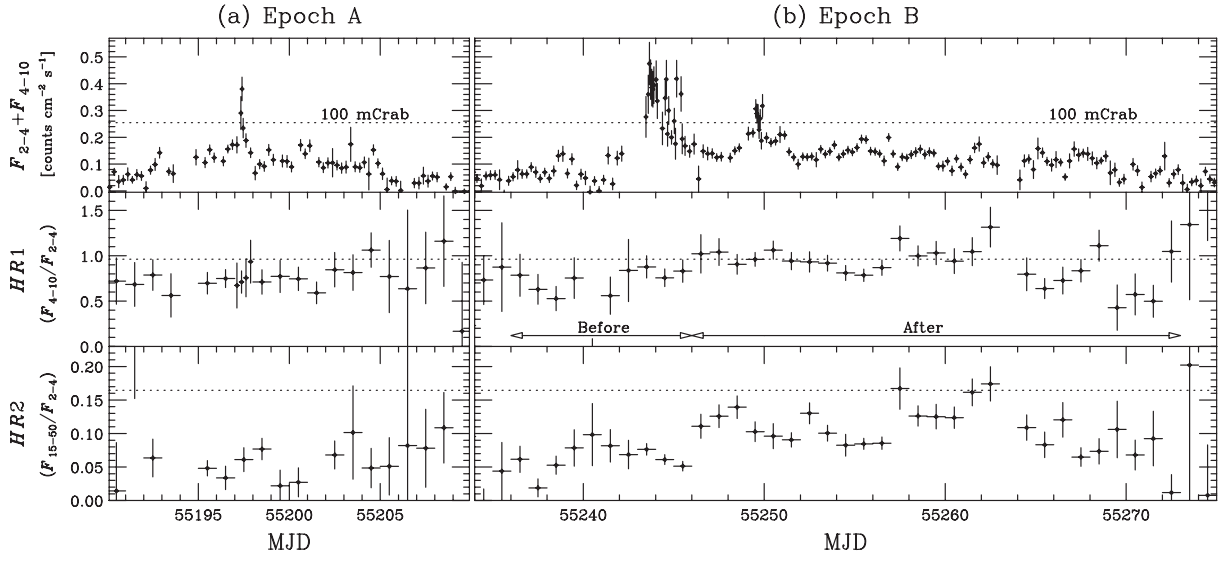

Fig. 2. Lightcurve of Mrk 421 during Epochs A (panel a) and B (panel b). The GSC 2–10 keV count rate, $F_{4-10}+F_{2-4}$ for a time resolution of 6 hours is shown at the top. A time resolution of 1.5 hour is adopted when the 6 hour averaged flux is higher than the 100 mCrab level (the dotted line). The center and bottom display the daily-averaged hardness ratios, defined as $HR1 = F_{4-10}/F_{2-4}$ and $HR2 = F_{15-50}/F_{2-4}$, respectively. For MJD = 55197 in panel (a), *HR1* is displayed every 6 hours. The hardness for the Crab-like spectrum with a photon index of $\Gamma = 2.08$ (Toor & Seward 1974) with a galactic absorption column density of $N_{\rm H} = 3.2 \times 21\,{\rm cm}^{-2}$ (Kalberla et al. 2005) is expressed by the dotted lines. The long and short arrows in the center of panel (b) define the phases before and after the decay of the Epoch B first peak (MJD = 55246), adopted in figures 3 and 4.

no significant increase in F_{15-50} was apparently found, while the object brightened in all energy ranges during Epoch B. The flare of Epoch A (MJD = 55197) was not covered with the Swift BAT, due to sparse sampling toward Mrk 421 during this period. In addition, the hardness variation between Epoch A and Epoch B (before the first peak) was found to be statistically insignificant, as we show below.

Figure 2 shows the 2–10 keV GSC lightcurve, $F_{2-4} + F_{4-10}$, during Epochs A and B, together with the hardness ratios, defined as $HR1 = F_{4-10}/F_{2-4}$ and $HR2 = F_{15-50}/F_{2-4}$. The lightcurve in Epoch A peaks at MJD = 55197.4, with a 2–10 keV flux of 120 ± 10 mCrab, averaged over 6 hours around the peak. Here and hereafter, the error represents the $1\,\sigma$ statistical one. The doubling time scales in the rise and decay phases of this flare were estimated to be $t_{\rm r} \lesssim 2 \times 10^4$ s and $t_{\rm d} \sim 2.5 \times 10^4$ s, respectively. During Epoch B, the source activity continued for about one month, and we found several flares in the lightcurve. The peak 2–10 keV flux of the first flare in Epoch B was measured at MJD = 55243.6 as 164 ± 17 mCrab on a 6-hour average. The decay time of this flare is derived as $t_{\rm d} \sim 1.4 \times 10^5$ s, a factor of 5–6 longer than that of the Epoch A flare. Due to a data gap with $\gtrsim 1$ day just before the peak seen in figure 2, we put only a loose upper limit on the rise time, as $t_{\rm r} < 1.3 \times 10^5$ s. The lightcurve exhibited the second peak at MJD = 55249.6 with a 2–10 keV flux of 108 ± 7 mCrab.

Utilising the daily averaged hardness ratio, we quantitatively investigated the spectral variation of Mrk 421 during Epochs A and B, as summarised in table 1. The hardness of the source was found to stay unchanged during Epoch A within the statistical uncertainties ($\chi^2/{\rm dof} = 7.3/18$ and $14.9/15$ for *HR1* and *HR2*, respectively). The average and standard deviation of *HR1* were derived as $\overline{HR1} = 0.74$ and $\sigma_1 = 0.10$, respectively, while those of *HR2* were calculated as $\overline{HR2} = 5.3 \times 10^{-2}$, and $\sigma_2 = 2.3 \times 10^{-2}$. Before the decay of the first flare in Epoch B (MJD = 55232–55245; corresponding to the arrows denoted as "Before" in figure 2), the object exhibited a hardness similar to that in Epoch A. No statistically significant spectral variation was observed during this phase ($\chi^2/{\rm dof} = 6.6/11$ and $7.4/9$ for *HR1* and *HR2*). After the decay of the Epoch B first flare (MJD = 55246–55275; indicated by the arrows with "After" in figure 2), the spectrum of the source seems to have hardened into $\overline{HR1} = 0.90$ and $\overline{HR2} = 10.0 \times 10^{-2}$, with a standard deviation of $\sigma_1 = 0.15$ and $\sigma_2 = 2.7 \times 10^{-2}$, respectively. In addition, the source hardness is found to have been variable ($\chi^2/{\rm dof} = 42.1/27$ and $73.8/27$ for *HR1* and *HR2*) during this period. Toward the end of Epoch B (MJD $\gtrsim$ 55264), the source appears to have recovered a hardness similar to those before the first peak (and hence those in Epoch A). In order to visualize these spectral variations associated with the flares,

Table 1. Summary of spectral variation of Mrk 421.

Epoch	A	B*	B†
$\overline{HR1}$‡	0.74	0.73	0.90
σ_1§	0.10	0.13	0.15
χ^2/dof	7.3/18	6.6/11	42.1/27
$\overline{HR2}$‡	5.3×10^{-2}	6.2×10^{-2}	10.0×10^{-2}
σ_2§	2.3×10^{-2}	1.1×10^{-2}	2.7×10^{-2}
χ^2/dof	14.9/15	7.4/9	73.8/27

* Before the first flare (MJD = 55232–55245).
† After the first flare (MJD = 55246–55275).
‡ Average of *HR1* and *HR2*.
§ Standard deviations of *HR1* and *HR2*.

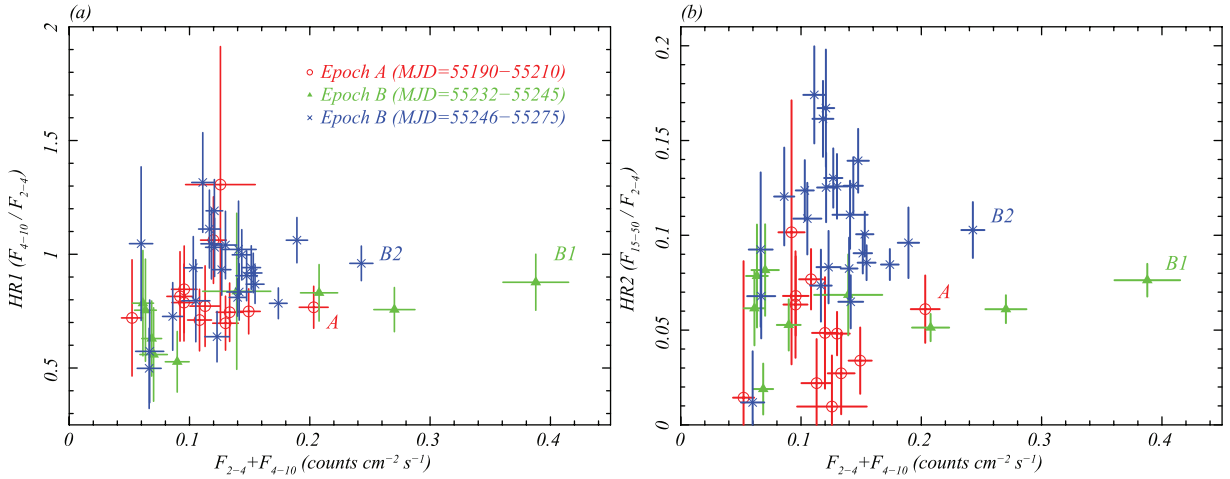

Fig. 3. *HR1* (a) and *HR2* (b) plotted against $F_{2-4} + F_{4-10}$, in a time resolution of a day. Only the data with $F_{2-4} + F_{4-10} > 0.05$ counts cm^{-2} s^{-1} are displayed. The error bars indicate the $1\,\sigma$ statistical errors. The circles show the data during Epoch A, while the triangle and crosses represent the Epoch B data before and after MJD = 55246, respectively (indicated the ranges with the two arrows in figure 2). The data points covering the peaks of the Epoch A flare, the first and second flares of Epoch B are respectively indicated with A1, B1, and B2, respectively.

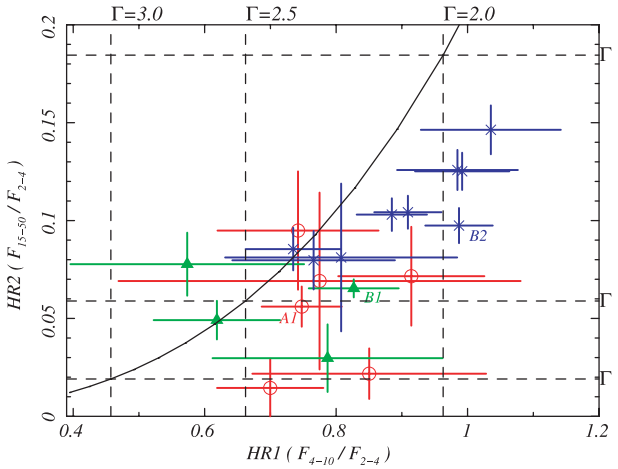

Fig. 4. Color–color plot between *HR1* and *HR2*, averaged over 3 days. The symbol notation same as figure 3 is adopted for the individual phases. Those covering the peaks of the Epoch A flare, the first and second flares of Epoch B are indicated by A1, B1, and B2, respectively. The error bars indicate the $1\,\sigma$ statistical errors. The dashed lines show the values of *HR1* and *HR2*, for the photon index of $\Gamma = 2.0$, 2.5, and 3.0, assuming that the galactic absorption column density of $N_{\rm H} = 1.9 \times 20\,{\rm cm}^{-2}$ toward Mrk 421 (Kalberla et al. 2005). If the spectrum is a straight PL in the 2–50 keV range, the data points lie on the solid line.

HR1 and *HR2* are plotted against the source X-ray intensity, $F_{2-4} + F_{4-10}$, in figure 3.

Figure 4 shows a color–color plot between *HR1* and *HR2* with a time resolution of 3 days. From this figure, we roughly evaluated the shape of the X-ray spectrum of Mrk 421. When a simple power-law (PL) model was assumed, the observed values of *HR1* corresponded to a 2–10 keV photon index of $\Gamma = 2$–2.5, as shown by the vertical dashed lines in figure 4. The systematic uncertainty in the photon index due to the current GSC response was estimated to be $\Delta\Gamma = 0.1$ (Nakahira et al. 2010). The figure also indicates a spectral softening from the MAXI GSC to the Swift BAT energy ranges.

3. Discussion

As shown in figures 1 and 2, at least the two active phases of Mrk 421 in 2010 January (Epoch A) and February (Epoch B) were extensively monitored with the MAXI GSC. The maximum 2–10 keV flux of the flare in Epoch A was derived as 120 ± 10 mCrab at MJD = 55197.4. During Epoch B, the MAXI GSC revealed a significant long-term activity of the source for nearly one month with a 2–10 keV flux of $\gtrsim 50$ mCrab, exhibiting multiple flares. This demonstrates a great advantage of the MAXI GSC for monitoring long-term variations of blazars. Especially, the first flare of Epoch B, of which the peak flux was measured as 164 ± 17 mCrab (MJD = 55243.6), is probably associated with a strong and variable activity in the VHE gamma-rays with the maximum VHE flux exceeding the 10 Crab level, detected on 2010 February 17 (MJD = 55244) by the VERITAS Observatory (Ong et al. 2010).

Since it was identified as the first extragalactic VHE γ-ray source in 1990s (Punch et al. 1992), Mrk 421 has been one of the most extensively studied blazars. As a result, a number of X-ray observations of the object were conducted with various X-ray observatories, including Ginga (Makino et al. 1992), ASCA (Takahashi et al. 1996, 2000; Tanihata et al. 2001, RXTE (e.g., Kataoka et al. 2001), XMM-Newton (e.g., Tramacere et al. 2007), Suzaku (Ushio et al. 2009), and so forth. Except for in significant X-ray flares, its 2–10 keV X-ray flux was reported to be typically below ~ 50 mCrab. Thanks to recent X-ray monitoring observations with Swift and the All Sky Monitor on board RXTE, strong X-ray flares were successively reported from the object; these include the flare in 2006 June with the 2–10 keV flux of ~ 85 mCrab (Tramacere et al. 2009), the flare in 2008 June with ~ 130 mCrab (Donnarumma et al. 2009) and the flare in 2009 December with ~ 100 mCrab (D'Ammando et al. 2009). It is important to note that the maximum X-ray flux in the first flare of Epoch B, measured with the MAXI GSC, is higher than any other previous results.

Therefore, we have concluded that MAXI GSC discovered the strongest X-rays from Mrk 421.

The color–color plot in figure 4 suggests that the MAXI GSC spectrum of Mrk 421 is roughly approximated by a PL with a photon index of $\Gamma = 2$–2.5. A convex curvature in the MAXI GSC and Swift BAT energy range, inferred from a comparison of *HR1* to *HR2* in figure 4, together with the previous determination of the synchrotron peak energy in Mrk 421 around the observed photon energies of $E_{\rm p} = 0.3$–5 keV (e.g., Tanihata et al. 2004; Tramacere et al. 2007; Ushio et al. 2009), implies a smoothly curved X-ray spectrum of the source.

In the case of HBLs, where the synchrotron peak frequency is located at the X-ray band, the timescale of the X-ray flux variation is thought to be controlled mainly by interplay between the following timescales (Kataoka 2000): the acceleration timescale of high-energy electrons, $\tau_{\rm acc}$; the radiative cooling time, $\tau_{\rm cool}$; and the light crossing time of the emission region, $\tau_{\rm crs}$. We, here describe all of the timescales in the observer's frame, after having converted those in the source rest frame, τ', as $\tau = \tau'/\delta$, in order to relate them directly to the observed timescales. For a significant flare to take place, the condition $\tau_{\rm acc} < \tau_{\rm cool}$ is required. Assuming that a flare is a single event, the rise timescale, $t_{\rm r}$, is expected to be determined by the longer of $\tau_{\rm acc}$ and $\tau_{\rm crs}$, while the longer of $\tau_{\rm cool}$ and $\tau_{\rm crs}$ is thought to dominate the decay timescale, $t_{\rm d}$. The soft X-ray lag, discovered with ASCA from Mrk 421 in the decay phase of an X-ray flare (Takahashi et al. 1996), was regarded to be produced by the energy dependence of $t_{\rm cool}$. In contrast, symmetric X-ray lightcurves with $t_{\rm r} \sim t_{\rm d}$, observed in day-scale flares from several HBLs, were interpreted to be shaped by $\tau_{\rm crs}$ (Tanihata et al. 2001).

Because the 2–10 keV MAXI GSC spectrum around the maximum of the flares was found to be consistent with $\Gamma \sim 2$, we regard that MAXI GSC observed the spectrum near the synchrotron peak frequencies. Therefore, we adopt the above argument about the flare timescale to evaluate the physical parameters of Mrk 421 in these flares. In the flare of Epoch A and the first flare of Epoch B, $t_{\rm d}$ was measured to be longer than $t_{\rm r}$. This indicates that $t_{\rm r}$ and $t_{\rm d}$ are dominated by different timescales with each other. As a result, we speculate the condition $\tau_{\rm cool} \gtrsim \tau_{\rm crs} \gtrsim \tau_{\rm acc}$ or $\tau_{\rm cool} \gtrsim \tau_{\rm acc} \gtrsim \tau_{\rm crs}$ in these flares, corresponding to $t_{\rm d} \sim \tau_{\rm cool}$ and $t_{\rm r} \gtrsim \tau_{\rm crs}$.

The synchrotron radiation usually dominates other cooling process in HBLs, including Mrk 421 (e.g., Kataoka 2000). Assuming isotropically distributed electrons in a randomly oriented magnetic field, the synchrotron cooling time scale is expressed as $\tau_{\rm cool} \sim 1.5 \times 10^3\, B^{-3/2} E_{\rm keV}^{-1/2} \delta^{-1/2}$ s (re-evaluated from Takahashi et al. 1996), with B, $E_{\rm keV}$, and δ being the magnetic field in G, the synchrotron photon energy in keV, and the beaming factor of the jet, respectively. We roughly evaluated a time-averaged magnetic field of $B \sim 4.5 \times 10^{-2}\ (\delta/10)^{-1/3}$ G in the flare of Epoch A, from the relation $t_{\rm d} \sim \tau_{\rm cool}$. Here, we assume the typical synchrotron photon energy of $E_{\rm keV} \sim 4$ keV, by averaging the X-ray spectrum of $\Gamma \sim 2$ in the MAXI GSC energy range (2–10 keV). This is barely consistent with the value determined from one-zone SSC modeling to the observed SED of Mrk 421 in previous observations within the systematic uncertainty ($B = 0.036$–0.44 G: Kino et al. 2002). A spectral softening or soft lag, due to the energy dependence of $\tau_{\rm cool}$, was unobservable within the MAXI GSC signal statistics. On the other hand, we can put an upper limit on the size R of the emission region as being $R \leq c\tau_{\rm crs}\delta/(1+z)$, where c is the speed of light. The condition $t_{\rm r} \gtrsim \tau_{\rm crs}$ gives $R \lesssim 6 \times 10^{15}\ (\delta/10)$ cm. This upper limit appears to be consistent with the values reported in previous strong X-ray flares (e.g., Donnarumma et al. 2009).

In a similar manner, we put a loose upper limit from $t_{\rm r}$ on the region size of the Epoch B first flare as $R \lesssim 4 \times 10^{16}\ (\delta/10)$ cm. The magnetic field, $B \sim 1.5 \times 10^{-2}\ (\delta/10)^{-1/3}$ G, is found to be weaker by a factor of ~ 3 than that in the Epoch A flare due to $t_{\rm d}$ being longer by a factor of 5–6, while the spectral softening [from $HR2 = (7.6 \pm 0.9) \times 10^{-2}$ at MJD = 55243 to $(5.1 \pm 0.7) \times 10^{-2}$ at MJD = 55245], suggested in figures 2 and 3 during the decay phase of the Epoch B first flare, appears to be related to the cooling process. We cannot deny a simple explanation for the possible weak magnetic field, that this flare was produced in a part of the jet different from that of the Epoch A flare with slightly different physical parameters and/or conditions, from the MAXI data alone. However, we regard that $t_{\rm d}$ is not actually determined by $\tau_{\rm cool}$ in the case of this flare, because the derived magnetic field is found to be out of the range of the typical value of Mrk 421 in previous studies (e.g., Kino et al. 2002). Based on a close examination of the X-ray lightcurve of HBLs obtained in the long-look ASCA and RXTE observations with a duration of $\gtrsim 1$ week, Tanihata et al. (2001) proposed a possibility that day-scale flares of HBLs are composed of short events with a timescale of $\sim 10^4$ s. A similar scenario is possible to account for the duration of the first flare of Epoch B ($t_{\rm d} \sim 1.6$ day), longer by a factor of 5–6 than that of the Epoch A flare. It is important to note that in order to validate the physical quantities estimated here, the examination of a multi-wavelength SED of Mrk 421, widely covering the synchrotron and IC components, and its variation are required, although it is beyond the scope of the present paper.

Within the framework of a simple one-zone SSC model, the peak energy and luminosity of the synchrotron component is thought to scale as $E_{\rm p} \propto B\gamma_{\rm p}^2\delta$ and $L_{\rm p} \propto B^2\gamma_{\rm p}^{2(2-\Gamma_{\rm p})}\delta^{2+\Gamma_{\rm p}} N_{\rm e} V$, where $\gamma_{\rm p}$, $\Gamma_{\rm p}(<2)$, $N_{\rm p}$, and V are the maximum Lorentz factor of the radiating electrons, the synchrotron photon index below $E_{\rm p}$ (assuming a simple PL spectrum), the normalization of the electron number density spectrum, and the volume of the emission region, respectively. From these scaling relations, a change in B, $\gamma_{\rm p}$, or δ is expected to be observed as a positive correlation between $E_{\rm p}$ and $L_{\rm p}$, while only $L_{\rm p}$ is anticipated to increase when $N_{\rm e}$ or V (corresponding to the total electron number) increase. The clear positive $E_{\rm p}$–$L_{\rm p}$ correlation, widely reported from Mrk 421 in previous observations (e.g., Tanihata et al. 2004; Tramacere et al. 2007), is thought to suggest a change in B, $\gamma_{\rm p}$, or δ.

The rise of $E_{\rm p}$ is thought to be recognised as rises in *HR1* and *HR2*. The hardness–intensity relation, shown in figure 3, suggests a slightly complicated spectral variation, which appears not necessarily to follow the $E_{\rm p}$–$L_{\rm p}$ positive correlation, especially in Epoch B. We notice that *HR2* becomes larger after the end of the first flare in Epoch B, as clearly shown in figure 2 and table 1. Although at the second

flare of Epoch B the source is fainter by $\sim 30\%$ than at the first one, its hardness [$HR2 = (10.3 \pm 1.5) \times 10^{-2}$ at MJD = 55249] is higher than that at the first flare [$HR2 = (7.6 \pm 1.5) \times 10^{-2}$ at MJD = 55243]. In addition, the hardest X-ray spectrum was realized, when the source flux was about one third of the maximum at the first peak [$HR2 = (17.4 \pm 2.5) \times 10^{-2}$ at MJD = 55262]. In order to interpret such a spectral behavior within a simple one-zone SSC framework, fine tuning of the physical parameters is required (e.g., a combination of the increase in B, $\gamma_{\rm p}$, or δ and the decrease in $N_{\rm e}$ or V). Otherwise, a multiple-zone/component SSC model (e.g., Ushio et al. 2009) could be preferred. For a detailed examination, it is necessary to investigate the multi-frequency SED and its variation.

Thanks to valuable comments from an anonymous referee, the present paper has been significantly improved. This research has made use of the MAXI data,[2] provided by the RIKEN, JAXA, and MAXI teams. We acknowledge support from the Ministry of Education, Culture, Sports, Science and Technology (MEXT) of Japan, by the Grant-in-Aid for the Global COE Programs "The Next Generation of Physics, Spun from Universality and Emergence" and "Nanoscience and Quantum Physics". This research was also supported by MEXT through Grant-in-Aids (19047001, 20041008, 20540230, 20244015, 21340043, 21740140, 22740120). We are grateful to Dr. M. Kino and Dr. M. Hayashida for their advice and assistance.

References

Band, D. L., & Grindlay, J. E. 1985, ApJ, 298, 128,
Barthelmy, S. D., et al. 2005, Space Sci. Rev., 120, 143
D'Ammando, F., Derri, M., Tramacere, A., Gehrels, N., Hoversten, E., & Krim, H. A. 2009, Astron. Telegram, 2295
Donnarumma, I., et al. 2009, ApJ, 691, L13
Isobe, N., et al. 2010a, Astron. Telegram, 2368
Isobe, N., et al. 2010b, Astron. Telegram, 2444
Kalberla, P. M. W., Burton, W. B., Hartmann, D., Arnal, E. M., Bajaja, E., Morras, R., & Poöppel, W. G. L. 2005, A&A, 440, 775
Kataoka, J. 2000, PhD thesis, The University of Tokyo
Kataoka, J., et al. 2001, ApJ, 560, 659
Kino, M., Takahara, F., & Kusunose, M. 2002, ApJ, 564, 97
Krimm, H. A. 2006, BAAS, 38, 374
Krimm, H. A., et al. 2009, Astron. Telegram, 2292
Makino, F., Fink, H. H., & Clavel, J. 1992, in Proc. 28th Yamada Conference: Frontiers of X-ray Astronomy, ed. Y. Tanaka & K. Koyama (Tokyo: Universal Academy Press), 543
Matsuoka, M., et al. 2009, PASJ, 61, 999
Nakahira, S., et al. 2010, PASJ, 62, L27
Negoro, H., et al. 2010, ASP Conf. Ser., 434, Astronomical Data Analysis Software and Systems XIX (San Francisco: ASP) in press
Ong, R. A., et al. 2010, Astron. Telegram, 2443
Padovani, P., & Giommi, P. 1995, MNRAS, 277, 1477
Punch, M., et al. 1992, Nature, 358, 477
Rodríguez-Pascual, P. M., et al. 1997, ApJS, 110, 9
Sembay, S., Warwick, R. S., Urry, C. M., Sokoloski, J., George, I. M., Makino, F., Ohashi, T.,& Tashiro, M. 1993, ApJ, 404, 112,
Takahashi, T., et al. 1996, ApJ, 470, L89
Takahashi, T., et al. 2000, ApJ, 542, L105
Tanihata, C., Kataoka, J., Takahashi, T., & Madejski, G. G. 2004, ApJ, 601, 759
Tanihata, C., Urry, C. M., Takahashi, T., Kataoka, J., Wagner, S. J., Madejski, G. M., Tashiro, M., & Kouda, M. 2001, ApJ, 563, 569
Tashiro, M., Makishima, K., Ohashi, T., Inda-Koide, M., Yamashita, A., Mihara, T., & Kohmura, Y. 1995, PASJ, 47, 131
Toor, A., & Seward, F. D. 1974, AJ, 79, 995
Tramacere, A., Giommi, P., Perri, M., Verrecchia, F., & Tosti, G. 2009, A&A, 501, 879
Tramacere, A., Massaro, F., & Cavaliere, A. 2007, A&A, 466, 521,
Tsunemi, H., et al. 2010, PASJ, 62, 1371
Ushio, M., et al. 2009, ApJ, 699, 1964

[2] ⟨http://maxi.riken.jp/top/index.php⟩.